OAK RIDGE NATIONAL LABORATORY LIBRARIES
3 4456 0554052 7

ORNL/TM-8226

ornl

OAK
RIDGE
NATIONAL
LABORATORY

UNION
CARBIDE

Initial Dynamic Simulation of an HTGR Sensible Energy Transport and Storage Plant

S. J. Ball N. E. Clapp, Jr.

OAK RIDGE NATIONAL LABORATORY
CENTRAL RESEARCH LIBRARY
CIRCULATION SECTION
4500N ROOM 175
LIBRARY LOAN COPY
DO NOT TRANSFER TO ANOTHER PERSON
If you wish someone else to see this report, send in name with report and the library will arrange a loan.
UCN-7969 (3 9-77)

OPERATED BY
UNION CARBIDE CORPORATION
FOR THE UNITED STATES
DEPARTMENT OF ENERGY

Printed in the United States of America. Available from
National Technical Information Service
U.S. Department of Commerce
5285 Port Royal Road, Springfield, Virginia 22161
NTIS price codes—Printed Copy: A03 Microfiche A01

This report was prepared as an account of work sponsored by an agency of the United States Government. Neither the United States Government nor any agency thereof, nor any of their employees, makes any warranty, express or implied, or assumes any legal liability or responsibility for the accuracy, completeness, or usefulness of any information, apparatus, product, or process disclosed, or represents that its use would not infringe privately owned rights. Reference herein to any specific commercial product, process, or service by trade name, trademark, manufacturer, or otherwise, does not necessarily constitute or imply its endorsement, recommendation, or favoring by the United States Government or any agency thereof. The views and opinions of authors expressed herein do not necessarily state or reflect those of the United States Government or any agency thereof.

ORNL/TM-8226
Dist. Category UC-77

Contract No. W-7405-eng-26

Instrumentation and Controls Division

INITIAL DYNAMIC SIMULATION OF AN HTGR SENSIBLE ENERGY TRANSPORT AND STORAGE PLANT

S. J. Ball N. E. Clapp, Jr.

Date Published - June 1982

NOTICE This document contains information of a preliminary nature. It is subject to revision or correction and therefore does not represent a final report.

Prepared by
OAK RIDGE NATIONAL LABORATORY
Oak Ridge, Tennessee 37830
operated by
UNION CARBIDE CORPORATION
for the
DEPARTMENT OF ENERGY

OAK RIDGE NATIONAL LABORATORY LIBRARIES
3 4456 0554052 7

CONTENTS

Page

ABSTRACT 1
1. INTRODUCTION 1
2. DESCRIPTION OF THE PROCESS 2
3. SETS PLANT DYNAMIC MODEL DESCRIPTION 5
3.1 Core Model 5
3.2 Circulator Model 5
3.3 Intermediate Heat Exchanger (IHX) Model 7
3.4 Helium-to-Salt Heat Exchanger Model 7
3.5 Salt Pumping Station Model 7
3.6 Process Heat Exchanger Model 7
3.7 Controller Model 7
4. SETS PLANT CONTROL SYSTEM PRELIMINARY DESIGN 8
5. EXAMPLE PLANT TRANSIENTS 11
6. CONCLUSIONS 18
REFERENCES 19
APPENDIX. SIMULATOR MODEL EQUATIONS 21

INITIAL DYNAMIC SIMULATION OF AN HTGR SENSIBLE ENERGY TRANSPORT AND STORAGE PLANT

S. J. Ball N. E. Clapp, Jr.

ABSTRACT

Dynamic models were developed for a General Atomic Company reference design of a high-temperature gas-cooled reactor sensible energy transport and storage (SETS) plant. The resulting computer code uses the IBM simulation language CSMP. The purpose of the program was to investigate the basic dynamic response behavior and controllability. The plant was found to have excellent inherent stability and control features.

1. INTRODUCTION

Sensible energy transport and storage (SETS) systems using the high-temperature gas-cooled reactor (HTGR) as a heat source are currently being considered by the Department of Energy, Gas-Cooled Reactor Associates (GCRA), and others as an economic source of industrial process heat. The use of thermal energy transport from large centralized plants is attractive because (1) the plants have lower unit costs as compared with smaller steam generation plants and (2) the plants may not have to be sited near populated areas.

This study uses as an example a General Atomic Company (GA) design of an 1170-MW(t) HTGR using an indirect cycle, with molten salt (HITEC) as the heat transport and storage medium. The purpose of the initial dynamic simulation is to investigate the inherent dynamic behavior and controllability of the plant. Further development would be required to simulate wider-range transients such as start-up and severe accidents.

2. DESCRIPTION OF THE PROCESS

The reference plant (Fig. 1) uses a conventional prismatic core HTGR rated at 1170 MW(t), which is ∿ 40% larger than the Fort. St. Vrain (FSV) reactor thermal output and has approximately the same helium primary-coolant outlet temperature (750°C). The purpose of the secondary helium loop is to provide isolation of the primary coolant from the energy transport and storage fluid, which is to be pumped off site to a variety of storage and process heat facilities. The high-temperature salt leaves the plant at 566°C (1050°F) and returns at 260°C (500°F), so clearly the transport system must be well insulated.

The control system design should be capable of accommodating both load flow and temperature changes, while minimizing the temperature perturbations in the core. Additionally, minimizing the electrical power required of the helium circulators is desirable (30 MW in each of the two loops).

The molten salt transport and storage system model is based on a United Engineers and Constructors design.[1] The salt loop consists of four sets of pump and storage units connected in series, with seven miles of piping between each station (Fig. 2). The process heat exchange device is arbitrarily assumed to be a salt-to-salt heat exchanger, where the load on the SETS plant is varied by changing the secondary-side flow of this heat exchanger. Other types of final heat exchangers could be used depending on the end use of the process heat.

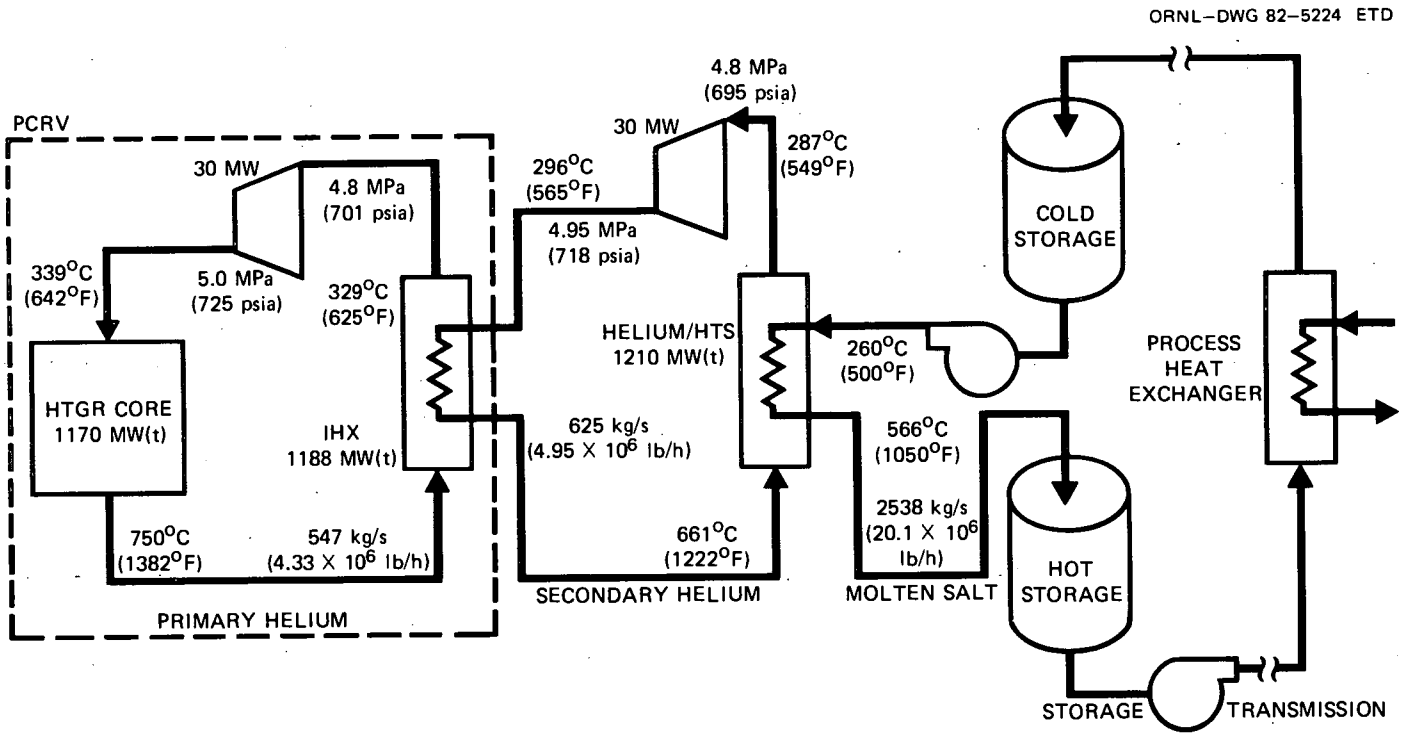

Fig. 1. Indirect HTGR — Sensible Energy Transport and Storage Plant (GA).

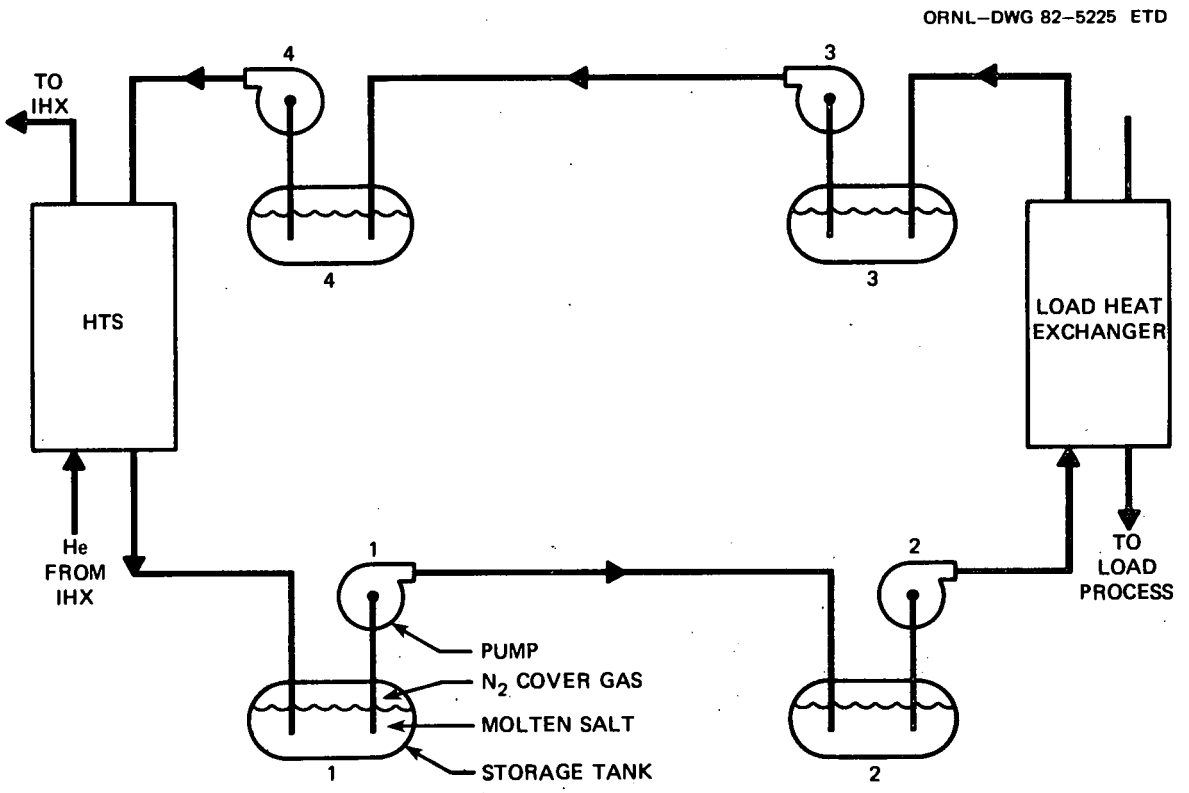

Fig. 2. Molten salt transport and storage system model.

3. SETS PLANT DYNAMIC MODEL DESCRIPTION

Much of the model development for the SETS plant was based on previous Oak Ridge National Laboratory work on gas-cooled reactor simulations. The IBM simulation language CSMP-3 was used, because the nonlinear differential equations describing the system can be solved efficiently with minimal programming effort. More details on each of the models listed can be found in the Appendix.

3.1 Core Model

The simulation of the prismatic core was based on a variation of the CORTAP code[2] that uses a single-channel thermal model plus a point-neutron kinetics approximation for the FSV core. While the CORTAP model typically uses 10 to 12 axial nodes and 3 to 4 radial nodes for each of the core segments, a simpler model could accurately represent typical FSV rod-jog perturbation test results.[3] Thus, the model used for the SETS reactor core uses a total of five axial sections, three for the active core and one each for the top and bottom reflectors. Each axial core section has a two-radial node characterization of the fuel plus moderator. Depending on the simulation being run, the user has an option of either including the six-delay group-neutron kinetics model or having the power "controlled" as an input.

3.2 Circulator Model

The model used for the SETS plant motor-driven circulators was also derived from a previous FSV simulation,[4] and the circulator head vs flow curves were scaled up from FSV data to correspond to the 1170-MW(t) reference plant conditions. Because the FSV circulators are steam-turbine driven, conversion from FSV to the SETS design case simply required removing the turbine section. The power required to drive the circulators is also calculated so that optimum control points can be derived.

The method of solution for the circulator operating point makes use of a technique that normalizes the head, flow, and speed parameters into a single-valued function. This function is approximated by the quadratic equation shown in Fig. 3. The advantage of this formulation is pressure drops around the loop are assumed to be proportional to flow squared, so the flow equation can be solved explicitly. The present system also includes a model for calculating pressure variations in the helium loops, but only for the case of constant inventory.

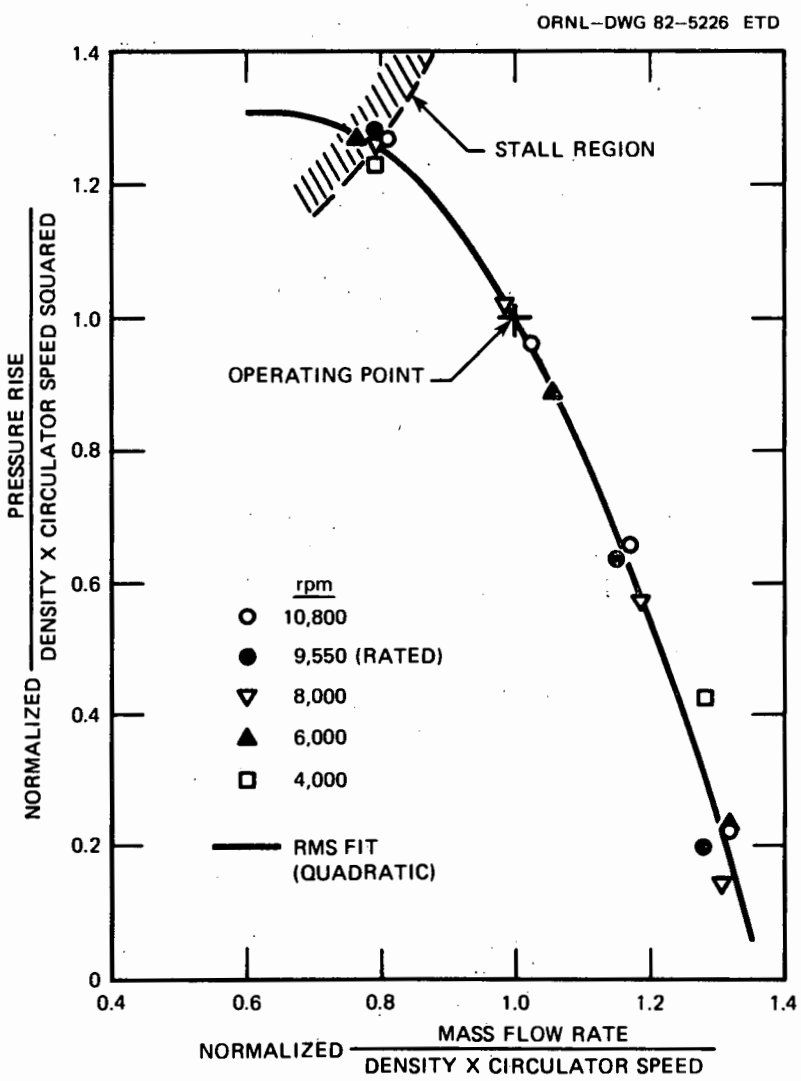

Fig. 3. Fort St. Vrain reactor helium circulator performance map (normalized).

3.3 Intermediate Heat Exchanger (IHX) Model

Design details of the IHX were not available when the model was being developed, so the simulation was derived from the rated performance characteristics. To develop a detailed dynamic model, a time-share program was written to take inputs describing the desired steady-state performance and calculate from them design parameters required for the dynamic model. The resulting model uses an 8-axial-section approximation that was determined necessary to simulate the distributed-parameter characteristics of the IHX over its expected operating range.

3.4 Helium-to-Salt Heat Exchanger Model

As in the case of the IHX, a special design code was written to obtain parameters for the helium-to-salt heat exchanger. In this case, a 15-section model was required. In the case of both the IHX and helium-to-salt exchangers, variable flow and temperatures are accommodated, and heat transfer variations are included as functions of flow. Approximate physical properties of HITEC molten salt are used.

3.5 Salt Pumping Station Model

Each of the four pumping stations is modeled by storage tank mass holdup and heat balance equations, pipeline hydraulics and holdup equations, and characteristic equations for the pumps. Control systems are included that maintain constant salt levels in each of the storage tanks.

3.6 Process Heat Exchanger Model

The salt-to-salt process heat exchanger, an arbitrary design, is primarily included just to simulate a variable process heat load. The reference model uses a four-section approximation.

3.7 Controller Model

A generalized model of a proportional-integral-derivative (PID) controller with an optional feed-forward signal is used for each of the closed-loop control systems.

4. SETS PLANT CONTROL SYSTEM PRELIMINARY DESIGN

Several plant control schemes could be used to provide control for the components of the SETS Plant. These schemes were tested using the SETS simulation to gain insight into the dynamic behavior of the plant and into the behavior of the control schemes. The control scheme selected for this study is defined by the following objectives:

1. Maintain a constant temperature at the outlet of the helium-to-salt heat exchanger by controlling the primary flow. The secondary flow of this heat exchanger should vary to follow load demand.
2. Maintain core exit temperature with varying coolant flow using control rods to vary reactor power. The rate at which the coolant flow may be changed is to be limited to reduce the variation in the temperature rise across the bundle.
3. Minimize the power consumed by the primary and secondary loop circulators to increase plant efficiency.
4. Maintain the exit temperature of the secondary side of the load heat exchanger by controlling the primary-side flow.
5. Maintain salt level in all tanks by controlling all the pumps in concert. This is accomplished by using the speed of the pump supplying salt to the load heat exchanger as the control signal for each of the other pumps. The control signal is altered by a signal developed by level changes.

A simplified plant control block diagram is shown in Fig. 4. This represents a preliminary scheme for meeting the control objectives as outlined, except that an optimization scheme for minimizing circulator power is not included. Core power is controlled by control rod manipulation to a level dictated by measured core outlet temperature as the input variable for feedback control and a feed-forward signal of measured load (salt flow). The core outlet temperature setpoint is a programmed linear function of salt flow, where a 100% decrease in salt flow would increase the setpoint by 56°C (100°F).

In a previous scheme, the primary circulator speed was varied to control the IHX secondary helium outlet temperature; however, that scheme led to controller interaction problems and was abandoned. In the present

ORNL–DWG 82–5227 ETD

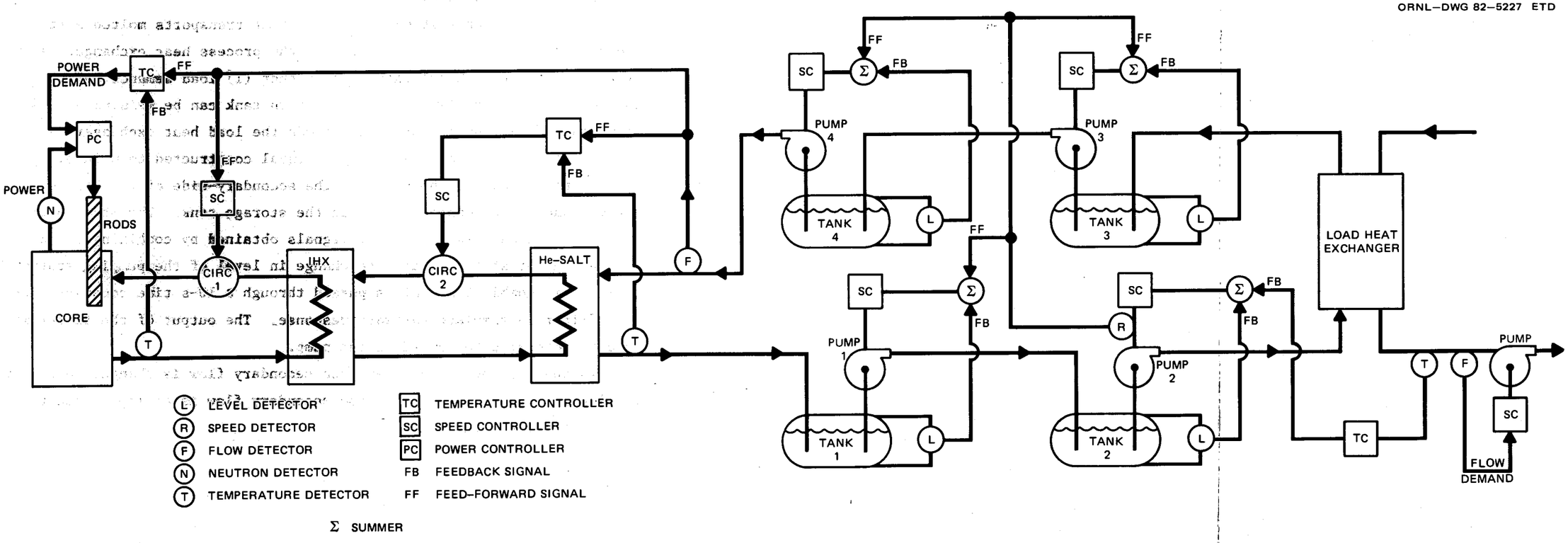

Fig. 4. SETS Plant simplified control system block diagram.

design, the primary circulator speed is set as a linear but limited-range function of salt flow. The final major control loop in the helium system is the control of the hot salt-to-storage temperature by means of varying the speed of loop 2 circulator. A linear, limited feed-forward load flow signal is also used here.

To include four stations in a loop that transports molten salt from the secondary helium heat exchanger to the process heat exchanger, a system is used to control each pump so that (1) load demands can be followed and (2) the level of salt in each tank can be maintained. As shown in Fig. 4, pumping station 2 feeds the load heat exchanger, and the speed of its pump is controlled by a signal constructed to maintain (1) a constant exit temperature on the secondary-side of the heat exchanger and (2) a constant level in the storage tank. The other pumping stations have pump-speed control signals obtained by combining the speed of the pump at station 2 and the change in level of the pumping station tank. This combined signal is passed through a 10-s time constant low-pass filter to simulate hardware response. The output of the filter is used to determine the speed of the pump.

In the load heat exchanger, the secondary flow is changed to follow the load. In this simulation, the secondary flow is an input used to represent a load demand.

5. EXAMPLE PLANT TRANSIENTS

Several example transients are shown to give an idea of the plant's inherent dynamic characteristics and controllability.

Figure 5 shows the inherent response of the system to a reactivity change (9.5¢ ramp decrease in 6 s) with no control actions taken and a fixed salt system heat load. In this model, the neutronics equations use typical FSV core parameters. Note that the inherent negative feedback mechanisms cause the responses to reach equilibrium quickly.

Figures 6 through 8 show a controlled plant response to a load perturbation (30% ramp decrease in salt flow in 100 s), where it can be seen

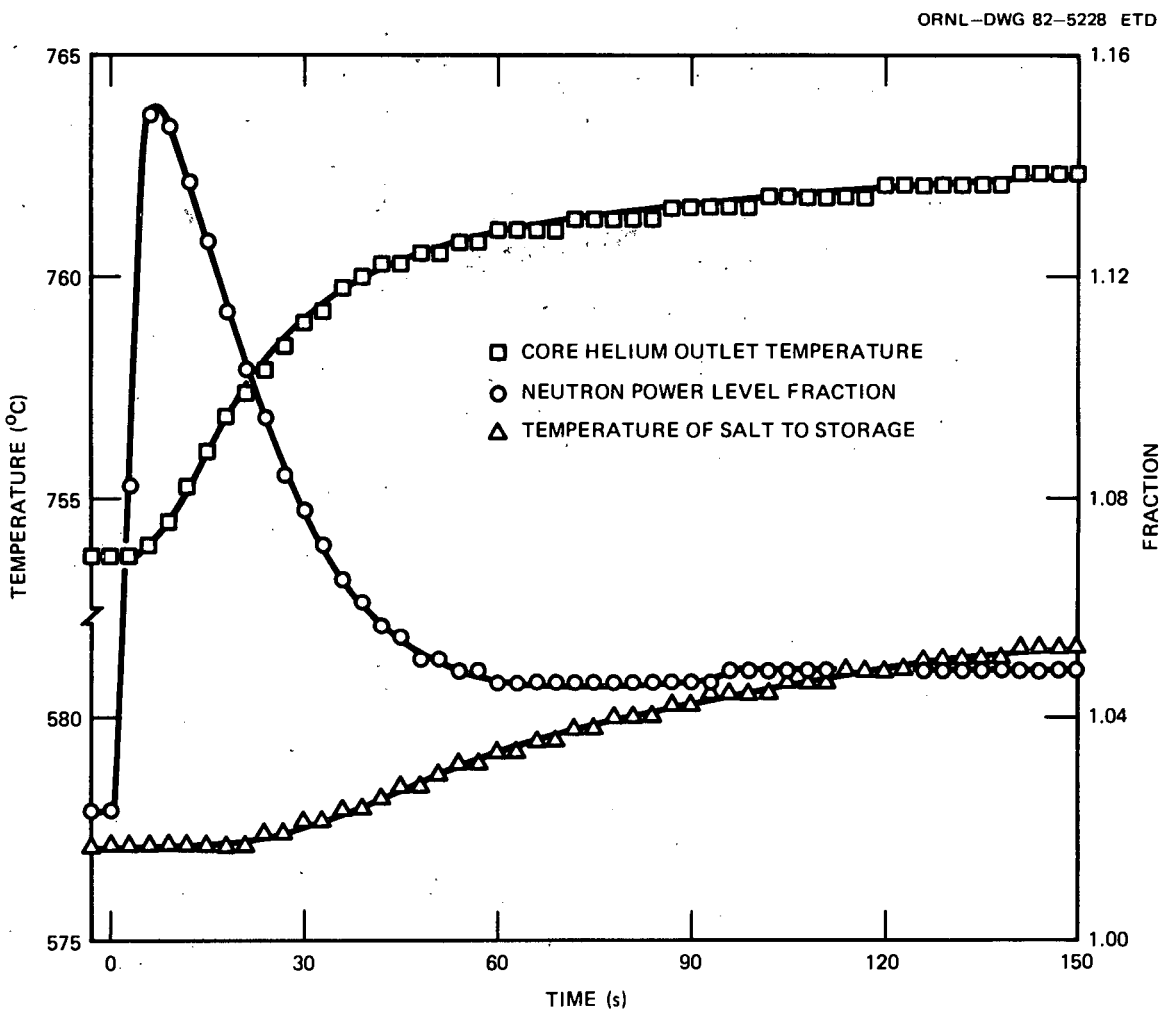

Fig. 5. SETS Plant simulator uncontrolled response to a +9.5¢ ramp reactivity input

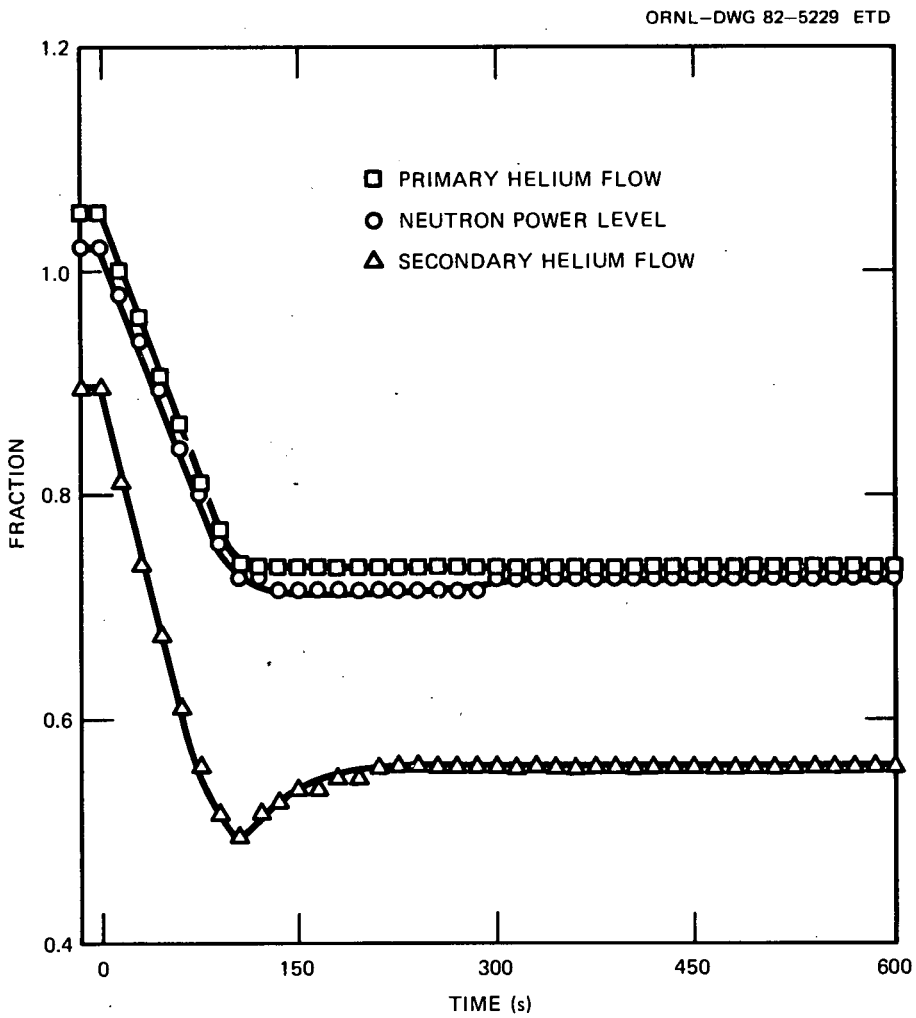

Fig. 6. SETS Plant simulator controlled response to a 30% ramp decrease in heat exchanger salt flow (load decrease).

that the load is followed very quickly and stably. Note that the primary helium flow (Fig. 6) is a pure ramp because it is affected only by a feed-forward signal from the load (salt) flow. The neutron power level control also uses a feed-forward signal from the load, but has a feedback component to control core outlet temperature. Likewise, secondary helium flow has both load feed-forward and feedback components, where the feedback signal maintains a constant salt-to-storage temperature. The results of the control actions are shown in Fig. 7, where the salt temperature is returned to its initial value in ∿300 s. Core helium outlet temperature is not quite settled out after 600 s at a new value determined by the programmed set

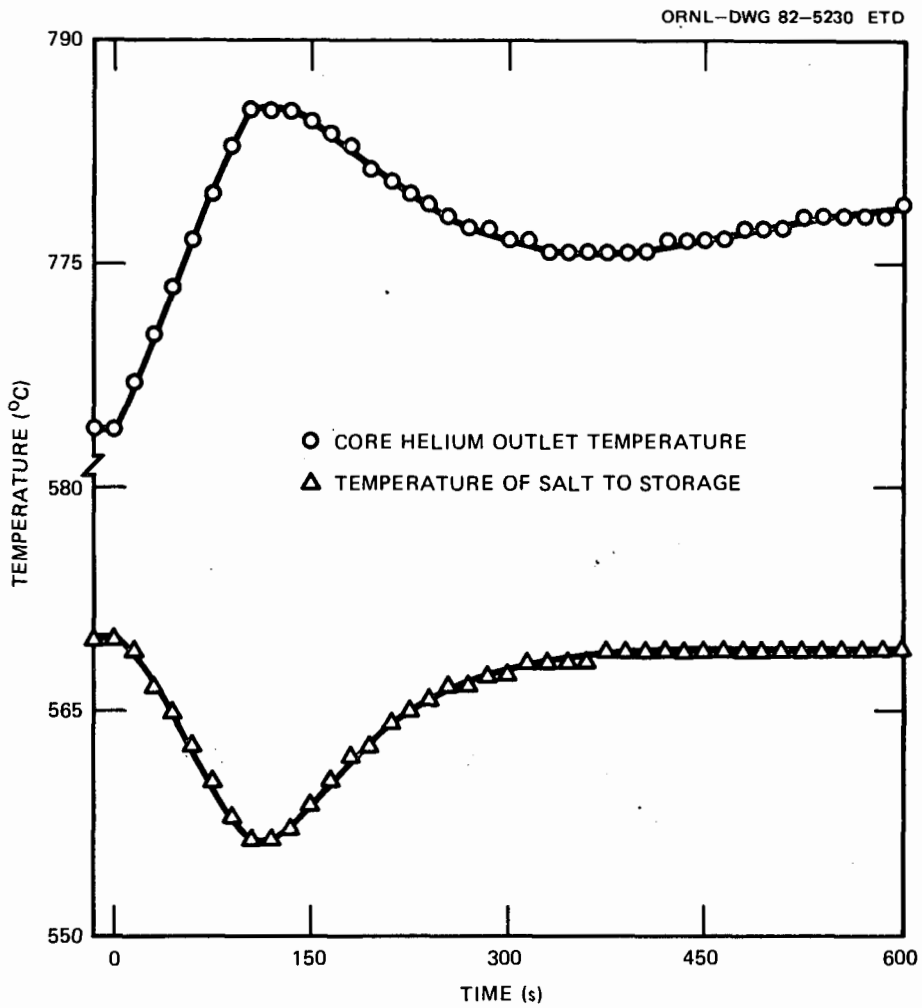

Fig. 7. SETS Plant simulator controlled response to a 30% ramp decrease in heat exchanger salt flow (load decrease).

point, which raises the temperature with decreasing load. Intermediate system temperatures (Fig. 8) for the 30% ramp load change show typical IHX behavior during a load reduction. The secondary helium inlet temperature decreases because the helium temperature closely approaches the salt temperature when the helium flow is reduced. The primary helium IHX outlet temperature rises because of both the higher primary inlet temperature and the reduced capacity of the IHX. Note that both flow rates were reduced, with the secondary flow reduction being much greater (Fig. 6). The reductions in circulator speeds with load for this transient resulted in a decrease in circulator power usage of 69%

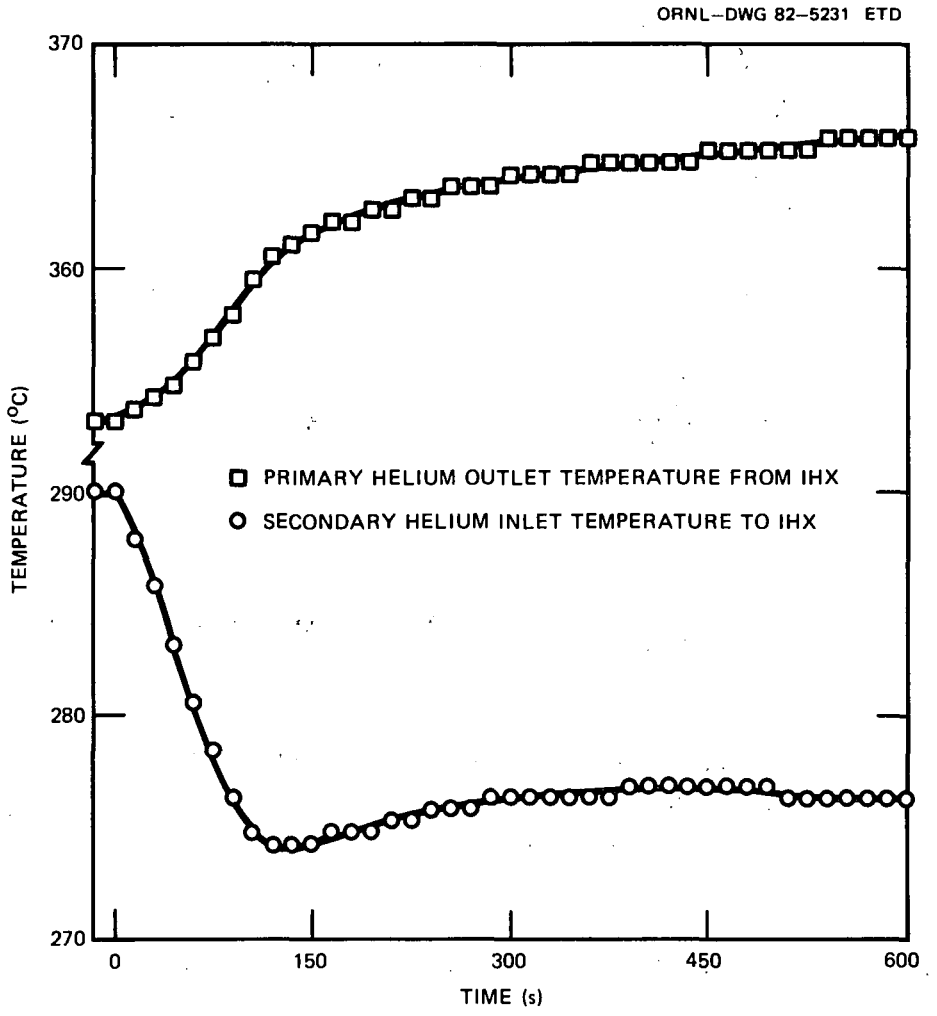

Fig. 8. SETS Plant simulator controlled response to a 30% ramp decrease in heat exchanger salt flow (load decrease).

(4635 MW) for the primary and secondary loops combined. In preliminary schemes to reduce circulator power consumption, the resulting low flows sometimes lead to instabilities, so eventual energy-optimization strategies would have to consider the dynamics as well as the statics.

Figures 9 through 11 show the response of the plant with the salt loop for a 20% step decrease in secondary flow of the final load heat exchanger. This is an effective change in load because the heat exchanger control has been set to control its primary-side flow to maintain a constant outlet temperature on the secondary side of the load heat exchanger. The

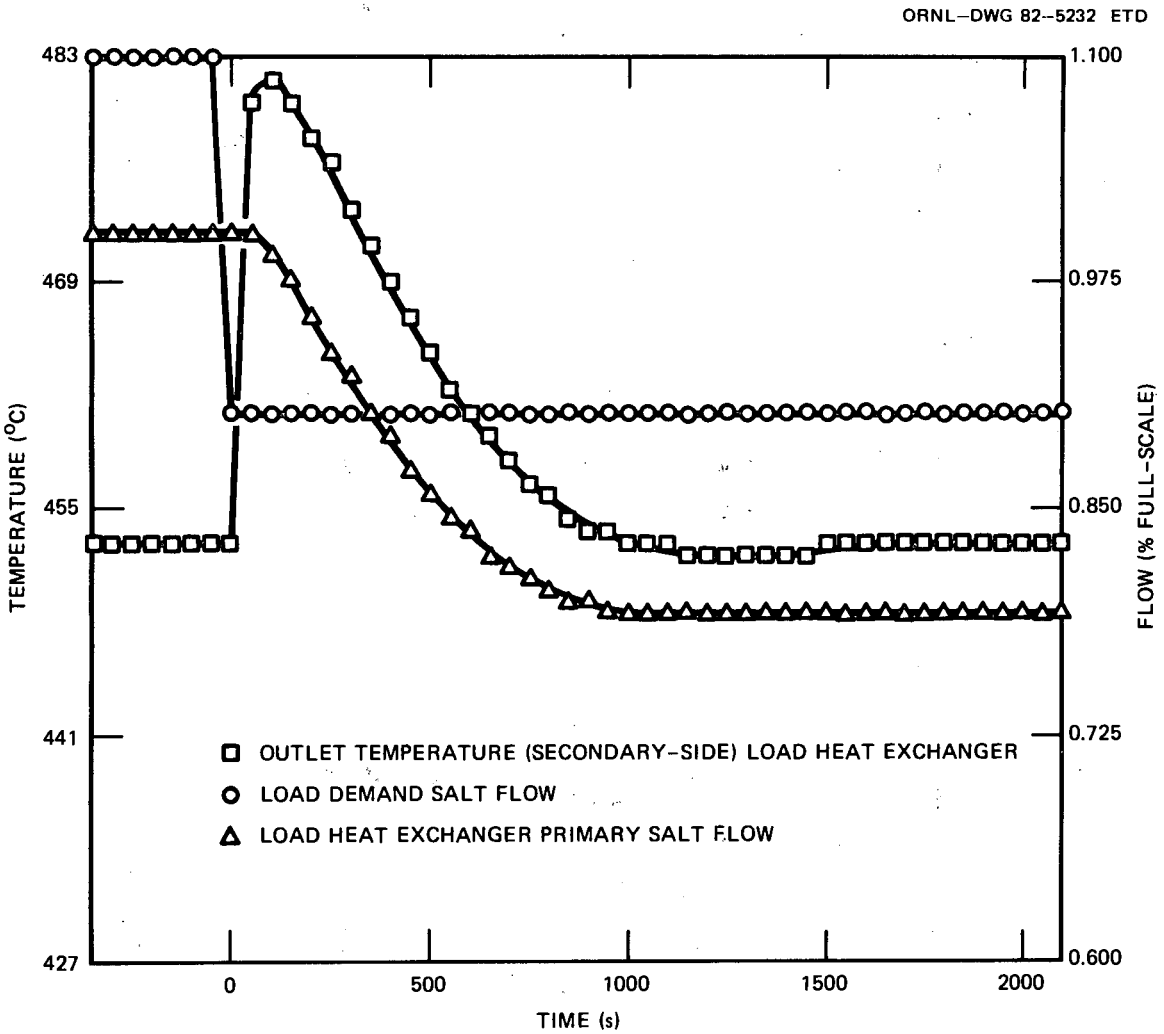

Fig. 9. SETS Plant simulator controlled response to a 20% step decrease in flow of the final load heat exchanger.

response shows that 1000 s is required to achieve the new operating condition after a change in load demand. To maintain the inventory in each of the storage tanks, the pump-speed control for tanks 1, 3, and 4 is set to follow the speed of the pump for storage tank 2. The speed of the pump for storage tank 2 is controlled to maintain a constant temperature at the secondary exit of the load heat exchanger. The circulator for helium flow through the reactor is controlled to follow the normalized flow out of storage tank 2. The reactor controls are set to maintain an exit temperature from the reactor that is dependent on the normalized salt flow on the primary side of the load heat exchanger.

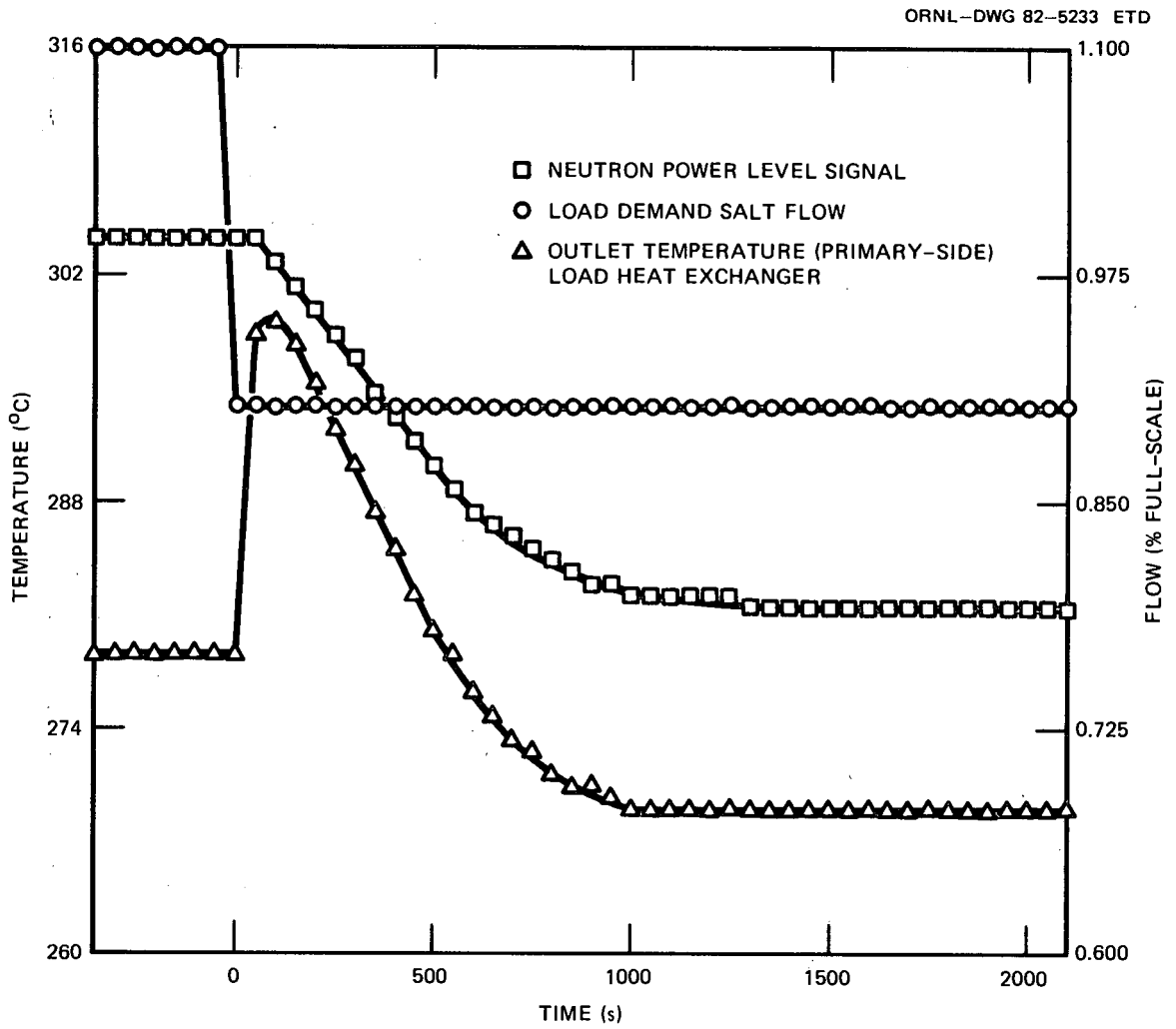

Fig. 10. SETS Plant simulator controlled response to a 20% step decrease in flow of the final load heat exchanger.

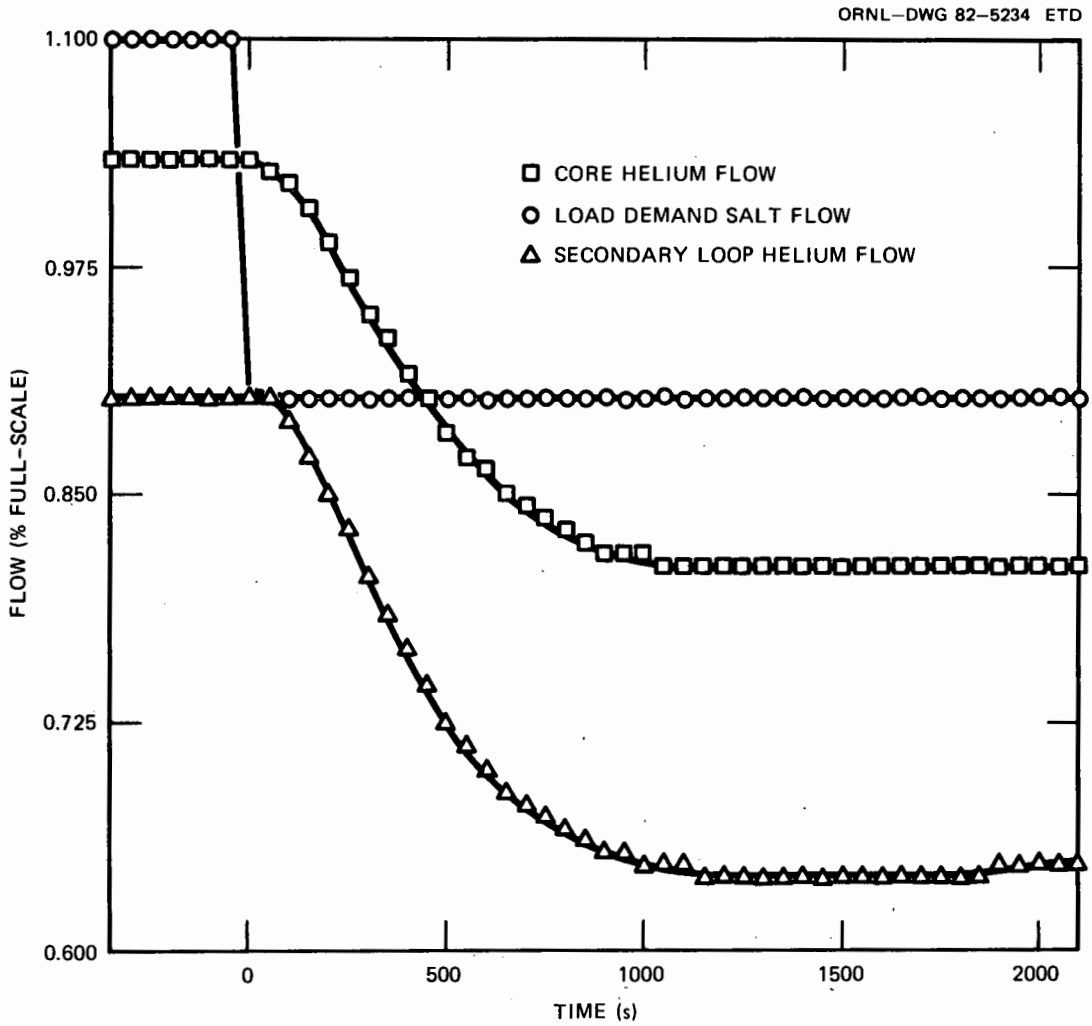

Fig. 11. SETS Plant simulator controlled response to a 20% step decrease in flow of the final load heat exchanger.

6. CONCLUSIONS

A preliminary simulation of the reference HTGR SETS Plant showed the system to have excellent inherent and controlled dynamic characteristics for the primary, secondary, and salt loop systems. The addition of the salt loop to the helium-cooled heat source significantly increased the response time of the system. The inventory controls on the salt loop were needed to prevent excessive loss of molten salt from the storage tanks. The manner in which the overall system responds to load changes is very sensitive to how well the inventory control system works. Further work on optimization and more sophisticated multiloop control schemes would be warranted if this plant design were to be considered further. When evaluating the relative advantages of different process heat supply systems, such factors as inherent stability and simplicity of control may regretfully be often overlooked. These factors should add significant credit to the SETS plant concept.

REFERENCES

1. United Engineers & Constructors, *HTGR Sensible Energy Transport and Storage System (SETS) Pipeline and Storage System Parametric Study*, Interim Report (May 1981).
2. J. C. Cleveland, *CORTAP: A Coupled Neutron Kinetics – Heat Transfer Digital Computer Program for the Dynamic Simulation of the HTGR Core*, ORNL/NUREG/TM-39 (January 1977).
3. S. J. Ball et al., *HTGR Safety Studies for the Division of Reactor Safety Research Quart. Prog. Rep. January–March 1980*, ORNL/NUREG/TM-397 (August 1980).
4. J. C. Cleveland et al., *ORTAP: A Nuclear Steam Supply System Simulation for the Dynamic Analysis of HTGR Transients*, ORNL/NUREG/TM-78 (September 1977).
5. S. J. Ball, "Approximate Models for Distributed Parameter Heat Transfer Systems," *Trans. Instrument Soc. Amer.* 3(1), 38 (January 1964).

APPENDIX. SIMULATOR MODEL EQUATIONS

A.1. Active Core and Reflector Models

The active core heat transfer model uses a cylindrical geometry two-radial-node approximation for each of three axial sections:

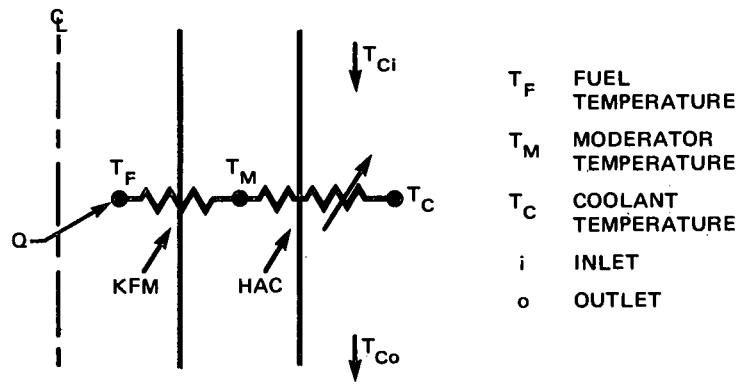

$$MCPF \frac{dT_F}{dt} = KFM\ (T_M - T_F) + PK \times APF \times N \quad , \tag{1}$$

$$MCPM \frac{dT_M}{dt} = KFM\ (T_F - T_M) + HAC\ (T_C - T_M) \quad , \tag{2}$$

and

$$T_C = (T_{Ci} + T_{Co})/2 \quad , \tag{3}$$

where

MCPF,M = effective fuel, moderator heat capacity for an axial section, Btu/°F,

KFM = fuel-to-moderator effective conductance, kW s^{-1} $°C^{-1}$ (Btu s^{-1} $°F^{-1}$),

PK = full-power heat input, kW (Btu/s),

APF = axial-power peaking factor,

N = normalized power level,

HAC = effective conductance term, moderator-to-coolant, kW s^{-1} $°C^{-1}$ (Btu s^{-1} $°F^{-1}$).

Note that the moderator-to-coolant conductance HAC has a fixed portion associated with the moderator conductance KADR and a variable conductance HA that is dependent on coolant flow:

$$HAC = (1/KADR + 1/HA)^{-1} \quad . \tag{4}$$

Because the gas transport times are small compared with overall core time responses, Eq.(3) and the energy balance equation for the gas can be considered as an instantaneous (algebraic) relationship:

$$(WC_p)_C \; (T_{Co} - T_{Ci}) = HAC \; (T_M - T_C) \quad , \tag{5}$$

where

$(WC_p)_C$ = coolant mass flow times specific heat, kW $°C^{-1}$ (Btu s^{-1} $°F^{-1}$).

The model for the reflectors is similar to that for the fuel except that only one radial node is used.

The neutronics model uses the basic space-independent kinetics equations with six delayed-neutron precursor groups:

$$\frac{dn}{dt} = \frac{\rho - \beta_T}{\Lambda} n + \sum_{i=1}^{6} \lambda_i C_i + s_o \; , \tag{6}$$

$$\frac{dC_i}{dt} = \frac{\beta_i}{\Lambda} n - \lambda_i C_i \; , \; i=1, 6 \; , \tag{7}$$

where

n = neutron population,

ρ = reactivity $\equiv k - 1$,

k = reactor multiplication factor = neutrons released per neutron lost,

β_i = fractional yield of delayed-neutron precursor group i,

$\beta_T = \sum \beta_i$,

λ_i = decay constant of precursor group i (s^{-1}),

Λ = prompt neutron generation time (s),

C_i = population of precursor group i,

s_o = neutron source generation rate (n/s),

t = time, s.

The values used for the nuclear parameters (β, λ, Λ, and fuel and moderator temperature feedback reactivity coefficients) were arbitrarily chosen for typical FSV beginning-of-cycle conditions.

A.2. Circulator Model and Loop Pressure Calculations

The circulator performance map that gives normalized head vs flow for several values of normalized speed (Fig. 3, Sect. 3.2) shows that a single-valued function is a good approximation. This function can be fit with a quadratic equation

$$Y \sim a_o + a_1 X + a_2 X^2 \ , \tag{8}$$

for

$$Y = \frac{(\Delta P/\Delta P_o)}{\rho N^2/(\rho N^2)_0} \ , \tag{9}$$

and

$$X = \frac{W/W_o}{\rho N/(\rho N)_o} \ . \tag{10}$$

The rms error of the fit was 0.047 (in units of Y).

The surge and fullflow limits correspond to X values of ~ 0.8 and 1.25, respectively, thus indicating a suitable method of monitoring these limits during operation; that is, for given (measured) values of N and ρ, one should ensure that

$$0.8 < W/\rho N < 1.25 \ . \tag{11}$$

Substitution of Eqs. (9) and (10) into Eq. (8) gives the circulator ΔP as a quadratic function of W:

$$\Delta P_{circ} = a_o \frac{\Delta P_o \rho N^2}{(\rho N^2)_o} + a_1 \frac{1/W_o}{\rho N/(\rho N)_o} W + a_2 \frac{1/W_o^2}{(\rho N)^2/(\rho N)_o^2} W^2 . \tag{12}$$

The loop pressure drop equations are approximated by

$$\Delta P_L \sim K_L (\overline{T}/\overline{P}) W^2 \ , \tag{13}$$

or

$$\Delta P_L \sim K_L' W^2 \ , \tag{14}$$

where

$\overline{T}, \overline{P}$ = effective absolute temperature and pressure of loop,

K_L' = a loop resistance parameter that accounts for temperature and pressure variations.

The calculation of K_L' involves finding effective flow resistances for several loop components in series.

For cases not involving loop depressurization, the solution for circulator flow is found by setting the loop and circulator ΔPs equal and solving Eqs. (12) and (14) as a quadratic function of the flow W.

The circulator power is calculated using a quadratic approximation of a performance map for the FSV circulator relating normalized horsepower to flow. Other power losses included are caused by bearing friction and rotor acceleration.

The nominal loop absolute pressure variation with constant loop inventory and varying loop temperatures is calculated by a two-point approximation, where

$$M_T = M_1 + M_2 \ , \tag{15}$$

and

$$\overline{P} = R\,\frac{M_1\overline{T}_1}{V_1} = R\,\frac{M_2\overline{T}_2}{V_2} \ . \tag{16}$$

Solving for $\overline{P}$ from Eqs. (15) and (16) gives

$$\overline{P} = \frac{RM_T}{\dfrac{V_1}{\overline{T}_1} + \dfrac{V_2}{\overline{T}_2}} \ .$$

A.3. Intermediate Heat Exchanger (IHX) Model

Modeling of the dynamics of gas-to-gas heat exchangers follows the development noted in Ref. 5. A typical section of a heat exchanger model is shown in Fig. A.1.

The energy equation for the tube metal $\overline{T}_m$ is

$$\frac{d\overline{T}_m}{dt} = \frac{1}{\tau_H}\,(\overline{T}_H - \overline{T}_m) + \frac{1}{\tau_c}\,(\overline{T}_c - \overline{T}_c) \ , \tag{17}$$

where

$\overline{T}_H$ = the hot fluid mean temperature;

τ_H = the hot-side tube time constant = $(MC_p)_m/(hA)_H$, s;

τ_c = the cold-side tube time constant = $(MC_p)_m/(hA)_c$, s.

Constants τ_c and τ_H are independent of length but vary as h changes with flow rate.

ORNL–DWG 80–4203A ETD

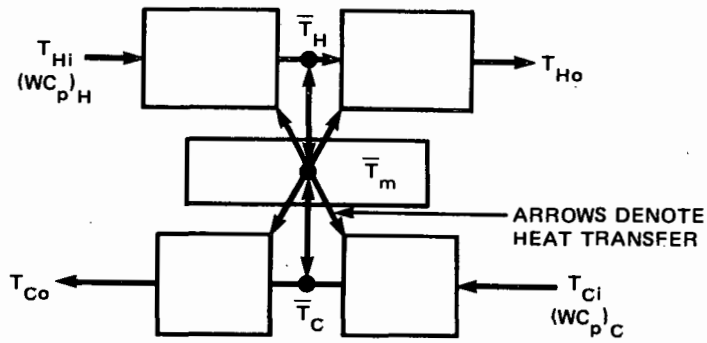

Fig. A.1. Typical heat exchanger section model.

Because the gas holdup times are small compared with the thermal time constants, an instantaneous (algebraic) energy balance relationship is appropriate for each gas side:

$$(WC_p)_H \, (T_{Hi} - T_{Ho}) = (hA)_H \, (\overline{T}_H - \overline{T}_m) \; . \tag{18}$$

This reduces to

$$T_{Hi} - T_{Ho} = n_H(\overline{T}_H - \overline{T}_m) \; , \tag{19}$$

where n_H is referred to as the "section length" for the hot-side gas $= (hA)_H/(WC_p)_H$, dimensionless. Likewise, for the cold side,

$$T_{Ci} - T_{Co} = n_C(\overline{T}_C - T_T) \; , \tag{20}$$

where $n_C = (hA)_C/(WC_p)_C$.

The tube lengths in each node are specified to be short enough so that arithmetic-mean temperature differences predict sufficiently accurate heat transfer rates; thus, for the coolant side

$$\overline{T}_C = 0.5 \, (T_{Ci} + T_{Co}) \; . \tag{21}$$

A similar equation applies to the hot side.

As the length of the section increases, n increases as well, and the accuracy of the arithmetic mean approximation worsens. Further, for $n > 2$, the initial response of T_{Ho} to a step change in T_{Hi} will be opposite in sign to the input change. Because this is nonphysical, the heat exchanger models are split up into enough sections so that, at minimum expected flow rates, both n_H and $n_C < 2$.

The value of n usually increases with decreasing flow rate because h is dependent on W, for example, if $h \propto W^{0.8}$, then $n \propto W^{0.8}/W^{1.0} = W^{-0.2}$.

In the MACRO model for a typical gas-to-gas heat exchanger section, the mean cool-side gas temperature is determined by combining Eqs. (20) and (21):

$$\overline{T}_C = \frac{T_{Ci} + (n_C T_T/2)}{1.0 + (n_C/2)} \quad . \tag{22}$$

Likewise, a similar equation is used for the hot-gas side by substituting subscript H for C.

A.4. Helium-to-Salt Heat Exchanger Model

The only difference between the models for the helium-to-salt and the gas-to-gas heat exchangers is that the coolant salt mass and holdup times are significant. The holdup in each section is approximated by two series nodes, which avoids the "wrongway response" problem encountered with single-node arithmetic-mean heat transfer models (i.e., if $T_{Ho} = 2\overline{T}_H - T_{Hi}$, a positive unit step change in T_{Hi} would cause T_{Ho} to change one negative unit, because $\overline{T}_H$ would not respond instantaneously).

The equations for the salt coolant side nodes are

$$\frac{d\overline{T}_C}{dt} = \frac{2}{t_C^*} (T_{Ci} - \overline{T}_C) + \frac{n_C}{t_C^*} (T_T - \overline{T}_C) \quad , \tag{23}$$

and

$$\frac{dT_{Co}}{dt} = \frac{2}{t_C^*} (T_C - T_{Co}) + \frac{n_C}{t_C^*} (T_T - \overline{T}_C) \quad , \tag{24}$$

where t_C^* is the salt holdup time in a section in seconds.

A.5. Salt Transport and Storage System Model

A salt storage tank is located at each pumping station. The storage tank has a reported volume of 1670 m^3 with a cross-sectional area of 130 m^2 and a height of 13 m. This gives a holdup time of 1160 s at full flow. For simulation purposes, the tank is assumed to be rectangular instead of cylindrical. The pumps are submerged in the salt in the storage tank. The pumping stations are connected by seven miles of pipe. The pipe is 11-cm ID for the hot leg and 13-cm ID for the cold leg, with full-flow pipe holdup times of 3400 and 4000 s, respectively. The equation that relates volume to inlet and outlet flow is

$$\frac{dL}{dt} = \frac{WI - WO}{\gamma A_T} \quad , \tag{25}$$

where

L = salt level,

A_T = cross-sectional area of tank,

γ = salt density,

WI = inlet flow,

WO = outlet flow.

The pipeline hydraulics equation, which includes the pump and seven miles of pipe, is written using an assumed linear relation between pump speed and pump head as

$$\frac{dW}{dt} = \frac{g\gamma A_p (L_1 - L_2)}{L_p} + \frac{gA_p}{L_p} (\Delta PP) - \frac{fW}{2d\gamma A_p} W \quad , \tag{26}$$

where

A_p = area of pipe,

L_1 = level of salt in tank salt is being pumped from,

L_2 = level of salt in tank salt is being pumped into,

L_p = length of pipe,

ΔPP = pump head,

g = acceleration due to gravity,

f = friction fractor,

W = mass flow rate in pipe,

d = pipe diameter.

Temperature effects are included by performing a heat balance on the storage tank and the pipe line. The storage tank is assumed to be a well-stirred tank having the exit temperature equal to the mean tank temperature. Then the tank heat balance can be represented by

$$\frac{dT_m}{dt} = \frac{WI}{\gamma A_T L} (T_i - T_m) , \tag{27}$$

where

T_m = mean tank temperature,

T_i = inlet temperature.

Some heat is assumed to be lost in the transmission pipe between storage tanks. This loss is assumed to be linearly related to flow rate with a 10 degree temperature drop at rated flow. This loss is computed at the exit of the tank using a first order lag time constant whose value is determined by the ratio of the weight of salt in the pipe to the mass flow rate.

These equations and assumed conditions are implemented with CSMP using a MACRO program describing the dynamic behavior of each pumping station. The dynamic effects included are the heat and mass balance of the storage tank and the hydraulic behavior of the pipe. The output values of the Macro program are the exit flow rate, the storage tank level, and the tank salt mean temperature. The required inputs are the

initial conditions of the three output values, the pump rotation speed, the level of the next storage tank, inlet flow, and inlet temperature. The transmission system is assumed to have a heat loss that is flow dependent. Because details of the transmission system are not known, a simple estimate was made on how the temperature would be affected by different flow rates. The dependence was assumed to be linear with flow rate with an 8.3°C (15°F) drop at zero flow and a 2.8°C (5.0°F) drop at full flow. The resulting temperature loss equation is

$$TSII = T_m + 5.5\ WN - 8.3\ , \tag{28}$$

where

TSII = pipe section inlet temperature,

WN = pipe section normalized flow.

This assumes that all the heat loss occurs at the pipe inlet. The transport lag is approximated by using a real pole function,

$$\frac{dT_i}{dt} = \frac{W}{MP}\ (TSII - T_i)\ , \tag{29}$$

where MP is weight of salt in pipeline.

A.6. Salt-to-Salt Heat Exchanger

The salt-to-salt heat exchanger is modeled by using a five-lump model for a typical section (Fig. A.1). The holdup in each section (hot and cold) is approximated by two series nodes and a single node to couple the hot and cold sections. A four-section model is used to simulate this heat exchanger.

A.7. Controller Model

The MACRO for a PID, three-mode controller has provisions for variable gain and time-constant settings and built-in gain limits on the integral and derivative stages of 100 and 10, respectively. These limits correspond to nominal values found in typical industrial controllers. The setpoint input is designed to enter the calculation downstream of the derivative stage. By changing the sign of the input gain term G, the user can choose to have either an increasing or decreasing output signal with an increasing error signal. Addition of ouput limits and feed-forward signals is left as a user option external to MACRO.

The frequency domain equation for the integral stage is that of a low-pass filter with a maximum (low-frequency) gain of 100 and a minimum (high-frequency) gain of 1.0. The time constant τ_I of the high-frequency break point is also known as the reset time, and $1/\tau_I$ is the reset rate.

$$\left.\frac{X_o}{X_i}\right|_{\text{integral}} = \frac{100\ (\tau_I S + 1)}{100\tau_I S + 1}\ , \tag{30}$$

where S is the Laplace argument.

The equation for the derivative stage is that of a high-pass filter with a maximum (high-frequency) gain of 10 and a low-frequency gain of 1.0. The time constant of the low-frequency break point, τ_D, is the derivative time.

$$\left.\frac{X_o}{X_i}\right|_{\text{derivative}} = \frac{\tau_D S + 1}{0.1\tau_D S + 1}\ . \tag{31}$$

The proportional stage, with gain = G, simply multiplies the error by G; the total controller output is the product of all three stages multiplied by the error signal.

ORNL/TM-8226
Dist. Category UC-77

Internal Distribution

1-5. S. J. Ball
6. O. W. Burke
7. N. C. Chen
8-12. N. E. Clapp, Jr.
13. J. C. Cleveland
14. J. C. Conklin
15. R. M. Harrington
16-17. P. R. Kasten
18. W. T. King
19. D. L. Moses
20. J. A. Mullins
21. F. R. Mynatt
22. T. W. Robinson, Jr.
23. J. P. Sanders
24. W. H. Sides
25. R. S. Stone
26. H. E. Trammell
27. ORNL Patent Office
28. Central Research Library
29. Document Reference Section
30-31. Laboratory Records Department
32. Laboratory Records, RC

External Distribution

33. C. N. Craig, Advanced Reactor Systems Department, General Electric Company, P.O. Box 508, Sunnyvale, CA 94086
34. Ron Foulds, Division of Accident Evaluation, RES, U.S. Nuclear Regulatory Commission, Washington, D.C. 20555
35. J. E. Fox, High Temperature Reactor Program, DOE, Washington, D.C. 20545
36. A. J. Goodjohn, General Atomic Company, P.O. Box 81608, San Diego, CA 92138
37. H. Gotschall, Gas-Cooled Reactor Associates, 33 North Torrey Pines Court, Suite 300, La Jolla, CA 92037
38. Richard Ireland, DOE Headquarters, 550 2nd St., Idaho Falls, ID 83401
39. George Kuzmycz, Division of Licensing, NRR. U.S. Nuclear Regulatory Commission, Washington, D.C. 20555
40. L. D. Mears, Gas Cooled Reactor Associates, 33 North Torrey Pines Court, Suite 300, La Jolla, CA 92037
41. G. A. Newby, High Temperature Reactor Program, DOE, Washington, D.C. 20545
42. G. R. Pflasterer, Advanced Reactor Systems Department, General Electric Company, P.O. Box 508, Sunnyvale, CA 94086
43. Director, Office of Nuclear Power Systems, DOE, Washington, D.C. 20545
44. Manager, DOE, San-San Diego, 110 West A Street, Suite 460, San Diego, CA 92101
45. Office of Assistant Manager for Energy Research and Development, DOE, P.O. Box E, Oak Ridge, TN 37830
46-178. Given distribution as shown in DOE/TIC-4500 under category UC-77 (Gas-Cooled Reactor Technology)

☆ U.S. GOVERNMENT PRINTING OFFICE: 1982-546-067/51